Comparisons of the MINOS Near and Far Detector Readout Systems at a Test Beam

A. Cabrera[*,f,1], P. Adamson[d], M. Barker[f], A. Belias[h], S. Boyd[g], G. Crone[d], G. Drake[a], E. Falk[j], P.G. Harris[j], J. Hartnell[*,f,h], L. Jenner[d], M. Kordosky[k], K. Lang[k], R.P. Litchfield[f], D. Michael[b,2], P.S. Miyagawa[f], R. Morse[j], S. Murgia[i], R. Nichol[d], T. Nicholls[h], G.F. Pearce[h], D. Petyt[e], D. Reyna[a], R. Saakyan[d], P. Shanahan[c], C. Smith[d], P. Symes[j], N. Tagg[f], J. Thomas[d], P. Vahle[k], A. Weber[f]

[a]*Argonne National Laboratory, Argonne, Illinois 60439, USA*
[b]*Lauritsen Laboratory, California Institute of Technology, Pasadena, California 91125, USA*
[c]*Fermi National Accelerator Laboratory, Batavia, Illinois 60510, USA*
[d]*Department of Physics and Astronomy, University College London, Gower Street, London WC1E 6BT, UK*
[e]*University of Minnesota, Minneapolis, Minnesota 55455, USA*
[f]*Subdepartment of Particle Physics, University of Oxford, Denys Wilkinson Building, Keble Road, Oxford OX1 3RH, UK*
[g]*Department of Physics and Astronomy, University of Pittsburgh, Pittsburgh, Pennsylvania 15260, USA*
[h]*Rutherford Appleton Laboratory, Chilton, Didcot, Oxfordshire, OX11 OQX, UK*
[i]*Department of Physics, Stanford University, Stanford, California 94305, USA*
[j]*Department of Physics and Astronomy, University of Sussex, Falmer, Brighton BN1 9QH, UK*
[k]*Department of Physics, University of Texas at Austin, Austin, Texas 78712, USA*

Abstract

MINOS is a long baseline neutrino oscillation experiment that uses two detectors separated by 734 km. The readout systems used for the two detectors are different and have to be independently calibrated. To verify and make a

---

[*]Corresponding authors, Tel.: +33 1 57 27 61 64; fax: +33 1 57 27 60 71

Email addresses: anatael@in2p3.fr (A. Cabrera), j.j.hartnell@sussex.ac.uk (J. Hartnell)

[1]Now at APC - Université Paris 7 Denis Diderot, 10, rue Alice Domon et Léonie Duquet, F-75205 Paris Cedex 13, France.

[2]Deceased

direct comparison of the calibrated response of the two readout systems, test beam data were acquired using a smaller calibration detector. This detector was simultaneously instrumented with both readout systems and exposed to the CERN PS T7 test beam. Differences in the calibrated response of the two systems are shown to arise from differences in response non-linearity, photomultiplier tube crosstalk, and threshold effects at the few percent level. These differences are reproduced by the Monte Carlo (MC) simulation to better than 1% and a scheme that corrects for these differences by calibrating the MC to match the data in each detector separately is presented. The overall difference in calorimetric response between the two readout systems is shown to be consistent with zero to a precision of 1.3% in data and 0.3% in MC with no significant energy dependence.

1. Introduction

The Main Injector Neutrino Oscillation Search (MINOS) is a long baseline, two-detector neutrino oscillation experiment that uses the NuMI neutrino beam at Fermilab [1]. The energy spectrum and flavour composition of the neutrino beam is measured at two detectors located 734 km apart: the Near detector (ND) at Fermilab and the Far detector (FD) at the Soudan Underground Laboratory in Minnesota [2]. MINOS is sensitive to neutrino oscillations in the region studied by the atmospheric neutrino experiments and has recently measured $|\Delta m^2| = 2.43 \pm 0.13 \times 10^{-3}$ eV^2 [3].

To control systematic errors, such as those that arise from uncertainties in neutrino flux and cross-sections, MINOS was designed as a two-detector experiment. This design allows a relative measurement to be made but it subsequently becomes necessary to ensure a precise inter-detector calibration of the energy scale. The MINOS ND and FD have a similar steel-scintillator structure but were instrumented with different readout systems. The driving factors for using different readout systems were the relatively small size and high event rate of the ND compared to the large size and low event rate of the FD. To investigate the effects of the two readout systems on the relative energy scale, test beam data were taken with the dedicated MINOS Calibration detector (CalDet) [4] that was simultaneously instrumented with both

readout systems. Specifically, differences arising from response non-linearity, photomultiplier tube crosstalk, and threshold effects were studied.

This paper quantifies the differences between the two readout systems and demonstrates how they can be controlled. In Sections 2 and 3 the experimental setup and the selection of the events used in the analysis are described. Section 4 outlines the calibration scheme and Section 5 details the uncertainties on the calibration. Comparisons of strip occupancy and PMT crosstalk for the two readout systems are given in Section 6. The results of the calorimetric response comparisons and the conclusions are given in Section 7 and Section 8 respectively. Further details of this analysis can be found in [5].

2. The MINOS Calibration Detector

The MINOS detectors are tracking-sampling calorimeters consisting of alternating layers of steel and scintillator planes. CalDet planes use 2.50 cm thick unmagnetised steel in contrast with the ND and FD that use 2.54 cm thick magnetised steel. In all three MINOS detectors, the plastic scintillator planes are made out of strips which are 1 cm thick and 4.1 cm wide. Successive scintillator planes are rotated by 90° to allow three dimensional event reconstruction. CalDet consists of 60 steel planes measuring 1×1 m square, interleaved with scintillator planes comprising of 24 strips of 1 m length. Light produced in the scintillator is captured by wavelength shifting (WLS) fibre optic cables. At two corners of each CalDet plane the WLS fibres from the 24 strips are brought together in a manifold. Additional fibre optic cables are then attached at the end of the manifolds to guide the light to multi-anode photomultiplier tubes (PMTs). The light output of CalDet was engineered to match the ND and FD by using long fibres: 6 m clear fibres on one end of the strips and 3 m green WLS fibres on the opposite end.

A schematic diagram showing the configuration of CalDet when it was simultaneously instrumented with both readout systems is shown in Fig. 1. The view of the detector shown is looking downstream at the first plane with successive planes following into the page. Each scintillator strip was read out at both ends: one end was instrumented with the ND readout system while the opposite end used the FD readout system. Successive planes alternate between the ND readout system being connected via clear fibres and the FD readout system by green WLS fibres and vice versa.
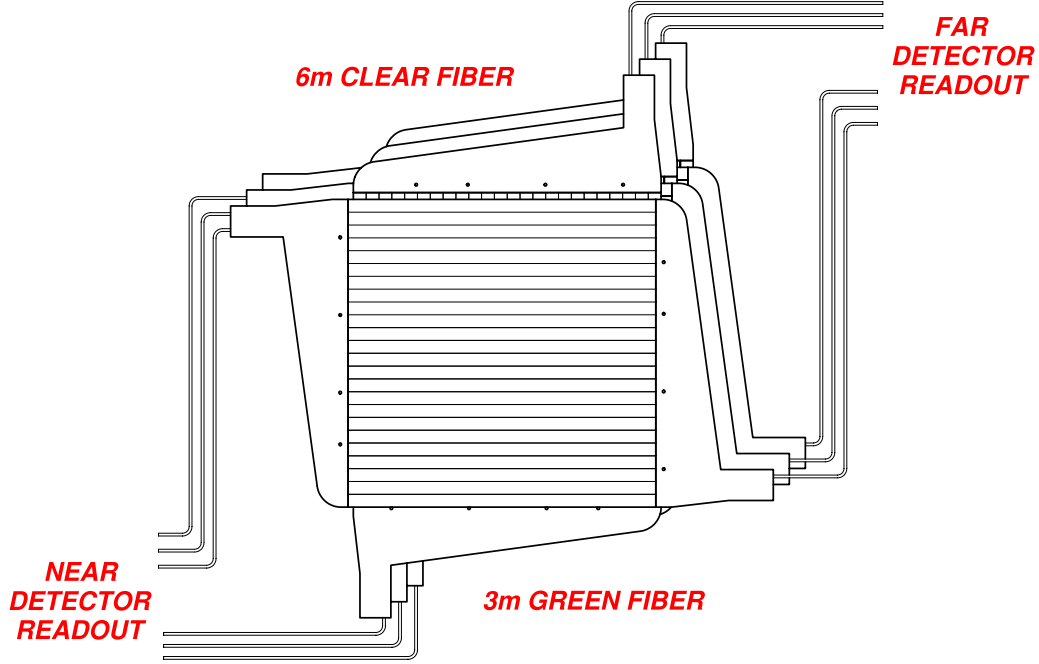
Figure 1: A schematic diagram showing the first 6 planes of CalDet. In the configuration shown, CalDet was simultaneously instrumented with both ND and FD readout systems. Clear fibres are connected to the two upper manifolds and green WLS fibres to the two lower manifolds.

The ND uses 64-anode Hamamatsu M64 PMTs [6] with a custom base divider ratio of 3-2-2-1-1-1-1-1-1-1-1-2-5 and electronics based on the QIE ASIC [7]. The FD readout system uses 16-anode Hamamatsu M16 PMTs [8] with a custom base divider ratio of 2.4-2.4-2.4-1-1-1-1-1-1-1-1-1.2-2.4 and electronics based on the VA ASIC [9].

The multi-anode PMTs used in MINOS have a single photocathode. The region of the cathode from which charge is focused on to a specific anode is called a pixel. The PMTs were housed in custom made boxes with optical routing that guided the light from individual strips to specific pixels. The routing pattern was designed such that neighbouring strips did not use neighbouring pixels. This was done to minimise the effect of crosstalk on pattern recognition. Crosstalk predominantly occurs on pixels next to the one illuminated due to leakage of photoelectrons before the first dynode [6, 8]. The optical routing of the FD readout system was such that three PMTs were fully utilised to readout two planes. The ND PMTs have 64 pixels, hence

4

only one PMT was required to read out two detector planes and 16 pixels remained unilluminated.

In the ND front-end electronics, the charge from each PMT pixel is integrated and digitised continuously at 53 MHz (every 18.8 ns) for up to several tens of μs with no dead-time. The digitisation is performed by a specialised ASIC, the QIE-chip. It splits the incoming signal into eight binary-weighted "ranges" and integrates the resulting fractional currents on capacitors in each range. A sample-and-hold circuit stores the integrated charge in each range. The QIE-chip then selects the first non-saturated range and passes its held voltage to the 8-bit ADC for digitisation. This combination of the 8 ranges with the 8-bit ADC gives the QIE-chip the same dynamic range as a 16-bit ADC but with an approximately constant fractional error across the entire dynamic range.

The QIE circuit does not provide a linear response by itself because each range has a different ADC offset and gain. A 16-bit DC current injection circuit is used to map the response of the chip. The results of that calibration are uploaded locally in a look-up-table and used during normal data taking. The calibrated output of the ND electronics is linear over the entire dynamic range to better than 0.5%. The stored data are processed once the acquisition period is complete. Pedestal subtraction and linearisation are performed for each channel via the look-up-table in a single step.

The FD readout system is based on the front-end ASIC VA32_HDR11 (short VA chip), developed in collaboration with the Norwegian company IDEA ASA. The chip includes a charge sensitive preamplifier, a shaper, sample and hold for each channel, and is followed by an analogue output multiplexer. The output from a selected channel can be switched to a differential output buffer, which drives a significant length of cable to a remote ADC. The ADC value is proportional to the integrated charge of the PMT pulse, but starts to saturate between 15 - 30 pC. Readout of the front-end electronics is triggered by a signal from the last dynode of each PMT and the dead time after each digitisation is 6 μs. This electronics was a cost effective choice for the low rate environment of a deep underground detector.

The amount of recorded data is reduced in both systems by recording hits above a readout threshold of about 1/3 of a photoelectron (PE). For the FD readout, this threshold is applied to the total integrated charge, while for the ND it is applied separately to each 18.8 ns integration sample.

2.1. The PS Test Beam and External Trigger

The results presented in this paper are based on data obtained by exposing CalDet in the T7 test beam in the East Experimental Hall of the 24 GeV/c CERN Proton Synchrotron (PS) [10]. The mixed composition beam of e, μ, π and p was operated between 0.6‑10 GeV/c. The beam line was instrumented with several Cherenkov counters to identify electrons and a time-of-flight (TOF) system to further aid particle identification. Control of the beam momenta spread ($\Delta p/p < 2\%$) and the instantaneous event rate (< 1 kHz) was achieved by adjusting the beam line collimators. For further details see [4, 11].

Synchronous readout of both systems was accomplished by an external trigger provided by the TOF counters. After a trigger, the ND and FD electronics were enabled for 376 ns and 1 μs time windows respectively, which was long enough to record individual events. In addition, for 50μs after each trigger, signals from the TOF system were suppressed to ensure that the electronics had ample time to complete the digitisation of the first event.

2.2. The Monte Carlo Simulation

The simulation results presented alongside the data in this paper use the MINOS Monte Carlo (MC) simulation. The MC is based on *GEANT3* [12] and is used to generate raw energy depositions (*GEANT* hits), which serve as the input to a C++ based detector response model. The response model includes the effects of light collection and propagation from the scintillator strips to the PMT photocathode as well as the PMT and the electronics.

The attenuation of light along the length of a strip is modelled as the sum of two exponential functions to give a short and a long attenuation component. Fits to both bench-top and cosmic ray data determined the lengths and relative contributions of the long and short components of the attenuation. In the simulation of the CalDet the approximation is made that every strip has the same short and long attenuation components. The variation in the light output of the strips and the gains of the PMTs are directly incorporated into the simulation by using the calibration constants determined by the detector calibration procedure (see Section 4).

3. Event Selection

The readout system comparison required separation of specific particle types and single-particle interactions in CalDet. Cuts to achieve this were

developed and are presented here. Positron and muon samples were chosen because they are efficiently identified with high purity and their energy loss mechanisms are well understood. When passing through iron at GeV-scale energies the positrons form a dense electromagnetic shower, which makes them ideal candidates for probing the full dynamic range of energy depositions expected for neutrino interactions in MINOS. The muons were used to probe some of the systematic errors of the calibration, their energy loss was close to minimum ionising and considerably more uniform through the detector than positrons.

Strict timing cuts were made to ensure that only events with single particle interactions were selected, and that events with multiple overlapping events from the test beam were rejected. This was done since rate of events at the FD is so low (about 1 Hz of cosmic ray muons) there is little to be gained from comparing the response for multiple overlapping particle interactions occurring at the same time ("pile-up" events). Further timing cuts were made to ensure that the single particle interactions were measured by both systems, since the length of time the two systems were enabled was different.

Positrons were selected by demanding the following: a TOF consistent with their velocity; a Cherenkov counter hit compatible with a single positron; coincidence in time of the TOF trigger and Cherenkov counter; and energy depositions only in the first 20 planes (to further reduce the number of pile-up events, specifically the case where an electron arrives in coincidence with a longer muon or pion).

High energy muons were selected by demanding: a TOF consistent with their velocity; no signal in the Cherenkov counter; a particle track crossing all 60 planes of the detector; and energy depositions consistent with a minimum ionising particle.

4. Calibration

The intrinsic calorimetric response of the ND and FD readout systems is different and thus it is necessary to calibrate their response independently. The readout system comparisons presented in this paper are dependent on the calibration and hence constitute a precise test of the calibration procedure's ability to remove the intrinsic response differences between the two readout systems.

The calibration of CalDet relies on an LED-based light injection system [13] and cosmic ray muons. A detailed description of the calibration techniques developed for MINOS using CalDet are given in [4]. A multi-stage procedure that converts the raw charge $Q_{raw}(i, t, x)$ measured by strip i at time t and position along the length of the strip x into a corrected signal Q_{cor} was used. Each calibration stage produced a numerical factor ("calibration constant"). Q_{cor} is defined by the product of $Q_{raw}(i, t, x)$ and the calibration constant from each stage:

$$Q_{cor} = Q_{raw}(i, t, x) \times D(i, t)$$
$$\times U(i) \times A(i, x) \times S,$$

where D, U, A and S refer to:

Drift Correction $D(i, t)$**:** To correct for temporal variations, data from the light injection system were used to track the response of each channel in the two readout systems[3].

Uniformity Correction $U(i)$**:** Cosmic ray muons that passed right through the detector were used to correct for differences in the overall light output of each scintillator strip. For the data presented herein, this calibration was done once and a 2% statistical precision was achieved.

Attenuation Correction $A(i, x)$**:** A correction for light attenuation along the length of strips was made separately for the horizontal and vertical strips. This attenuation correction had to be made because the test beam particles hit the detector up to 2 cm away from the centre of the 1st plane depending on their momentum and particle type. Deviations from the centre of the detector meant that, without correction, the response measured by one readout system was systematically low or high with respect to the other.

MC simulations of positrons striking the detector in a number of different positions were used to compute overall attenuation correction factors used for both data and MC. A correction factor of $\pm 0.2\%$/cm for both horizontal and vertical strips was applied separately to the two readout systems to give the response as if the positrons struck the centre of the plane.

Signal Scale Correction S**:** Stopping muons are used to set an overall energy scale [14]. A muon energy unit (MEU) is defined, which corresponds to the energy deposited by an approximately 0.8 GeV muon passing per-

---

[3]The light injection data were also used to determine the gain of each channel but this information was not directly used in determining Q_{cor}.

pendicularly through a 1 cm thick MINOS scintillator plane (the average absolute energy deposition by such a muon is approximately 2 MeV). An energy deposition of 1 MEU yields about 4 PE per strip-end. The same scale factor is used for both readout systems; i.e. the MEU scale has no impact on the relative response comparison. However, the MEU scale is defined to allow calorimetric response comparisons among the three MINOS detectors.

5. Calibration Uncertainties

5.1. Drift Correction

The drift in the absolute response of the two readout systems with time was of the order of several percent [4] over several weeks of running. This was mostly due to large temperature variation in the experimental area of up to 10°C. However, the absolute temperature dependence of the two readout systems was found to be almost identical and hence the error on the relative response was a negligible 0.1%. This was determined from 1 GeV/c test beam positron data sets taken at regular intervals.

5.2. Uniformity Correction

The performance of the uniformity correction is illustrated in Fig. 2 by plotting the average calibrated response per plane for test beam muons with momentum greater than 2 GeV/c. These muons travel through the detector by entering at the centre of the first plane and exiting within a 25 cm radius of the last plane's centre. The FD and ND readout systems have a 2.4% and 3.0% spread in response from plane to plane respectively, which demonstrates the size of the systematic uncertainties on the uniformity correction.

5.3. Non-Linearity Measurements

The response of the readout system to light from the scintillator is not perfectly linear due to non-linearities in the PMT and electronics response. To incorporate the correct level of non-linearity into the MC simulation a data driven approach was taken. The light-injection system was used to measure the average non-linearity (1-measured/expected) of all readout channels for the two systems separately. These measurements were then used in the MC simulation to induce a non-linear response.

The data from the light-injection system are shown in Fig. 3, where the non-linearity of each readout system is plotted as a function of the number of expected photoelectrons. PIN photodiodes that measured the quantity of
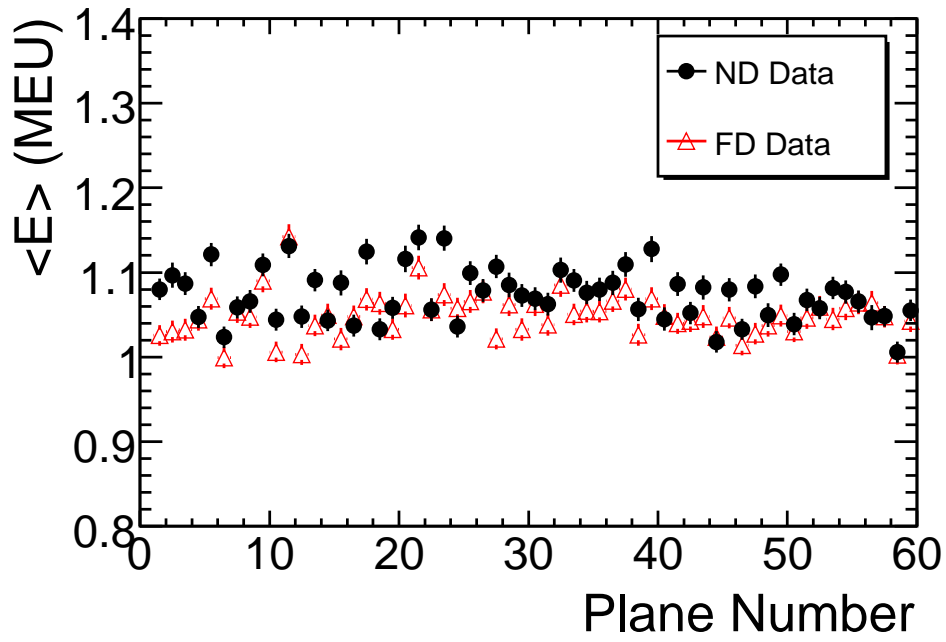
Figure 2: Average calibrated energy deposited versus plane by >2 GeV/c test beam muons. The error bars show the statistical error, thus the jitter from point to point is indicative of systematic error in the uniformity calibration. The observed response spread of the points is 2.4% and 3.0% for the FD and ND readout systems respectively.
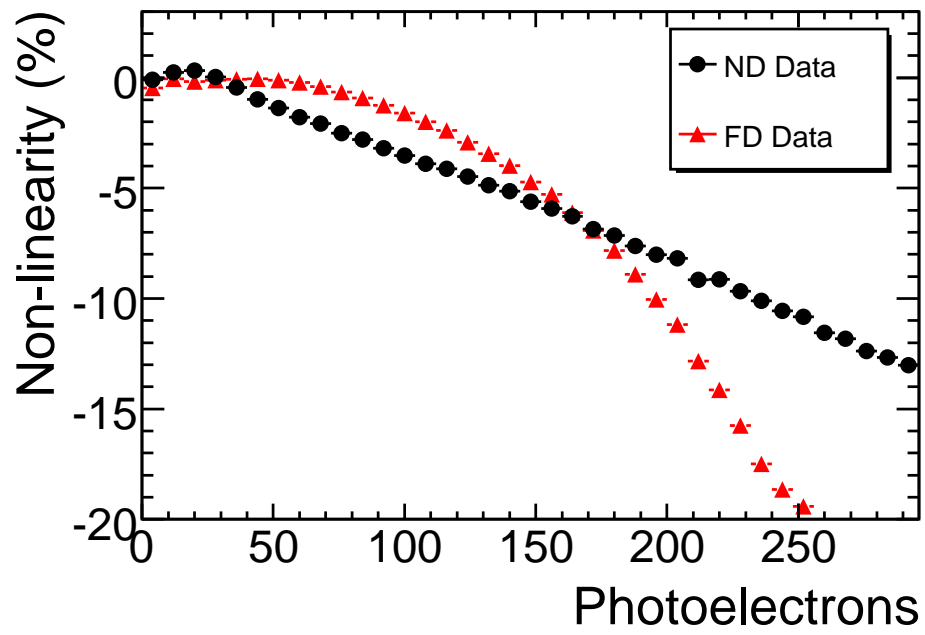
Figure 3: Average non-linearity of the ND and FD readout systems versus the number of PE injected by the light injection calibration system. The difference in the non-linearity between the two readout systems can be clearly seen.

injected light with a high degree of linearity were used to determine the expected number of photoelectrons. The ND PMTs are more non-linear than the FD PMTs. A fit to the CalDet data gave -0.05%/PE and -0.03%/PE deviations from linearity for the ND and FD PMTs respectively [5]. However, as can be seen from Fig. 3, the PMT non-linearity does not explain all the data. The shape of the overall (PMT plus electronics) readout system non-linearity is quite different for the two cases. This occurs because of a saturation effect in the FD electronics that becomes significant for signals above about 100 PE. Beyond 200 PE the FD readout system can be seen to become significantly more non-linear than the ND system. Overall, the non-linearities of both readout systems are the same to within 2% up to about 200 PE.

No correction for non-linearity was applied to the data or the MC. This approach was taken in order to investigate and understand the relative effects of the non-linearity. Furthermore, by considering this worst case scenario it is possible to set a maximum error on the relative energy calibration between the two detectors. This maximum error can then be reduced by performing a non-linearity calibration in the Near and Far detectors. However, since the non-linearity of the two readout systems is similar (see above), the systematic error on the relative energy scales is expected to be small for the range of energy depositions relevant to MINOS.

6. Strip Occupancy and PMT Crosstalk Comparison

The strips that register a response for a given particle interaction is not always the same for the two readout systems. Differences in strip occupancy[4] can arise due to PMT crosstalk, the average number of photons striking the PMTs and readout thresholds. The effect of crosstalk on the strip occupancy can be clearly demonstrated by using test beam muons since they only strike the central few strips all along the length of the detector. Fig. 4 shows the relative strip occupancy for test beam muons with momentum greater than 2 GeV/c. The central peak is mostly formed from strips that the muon actually passed through. In contrast, the peaks towards the edges of the detector (strip number 0 - 3 and 20 - 23) are dominated by crosstalk hits. The strip occupancy at the detector edges is different between the two readout

---

[4]Strip occupancy is a count of the number of times a specific strip is hit, normalised by the total number of strips registering a hit.

systems due to the different cabling configurations and PMTs used. Overall, it can be seen that the strip occupancy is well reproduced by the MC for both readout systems.

In addition to studying the strip occupancy, detailed studies were made of the crosstalk at the PMT level. The crosstalk arises primarily when photoelectrons injected on one pixel leak into the dynode chains of neighbouring pixels. Thus, crosstalk can be quantified as $Q_{Neighbour}/Q_{injected}$, where $Q_{injected}$ is the charge on the anode of the pixel where light was injected, and $Q_{Neighbour}$ is the charge that appears on the anodes of the neighbouring pixels. In-situ measurements of this crosstalk using muons in CalDet gave values of $5.2\pm0.1\%$ and $4.8\pm0.1\%$ for the FD and ND respectively [5]. However, since 16 of the 64 pixels on each ND PMT were not used, the observed crosstalk fraction associated with strips dropped to $3.2 \pm 0.1\%$, consistent with expectations[5].

7. Calorimetric Response Comparison

The calorimetric response of the readout systems are compared in two distinct ways: a "hit-by-hit" comparison and an "event-by-event" comparison. In the hit-by-hit comparison the difference in the response from the two ends of individual strips is taken. For the event-by-event comparison, it is the sum total of the response of all the strip-ends read out by one system that is compared with the sum total of the response of all the strip-ends read out by the other system. In this paper, the differences are characterised by a relative response asymmetry, $A_{\mathcal{N}/\mathcal{F}}$. In general form, $A_{\mathcal{N}/\mathcal{F}}$ is written as

$$A_{\mathcal{N}/\mathcal{F}} \quad = \quad \frac{\mathcal{N} - \mathcal{F}}{\frac{1}{2}(\mathcal{N} + \mathcal{F})},$$

where $\mathcal{N}$ and $\mathcal{F}$ are the calorimetric response of the ND and FD readout systems respectively. The data are presented here as the average hit-by-hit asymmetry, $< A_{\mathcal{N}/\mathcal{F}}^{Hit} >$, and as the average event-by-event asymmetry, $< A_{\mathcal{N}/\mathcal{F}}^{Event} >$. It should be noted that in order for a comparison to be made in the hit-by-hit case, a response above threshold on both ends of the strip

---

[5]The naive expectation is for the crosstalk associated with strips to drop by 16/64 to 3.6%. However, effects arise from exactly which 48 of the 64 pixels are connected to strips since some pixels receive more crosstalk than others.
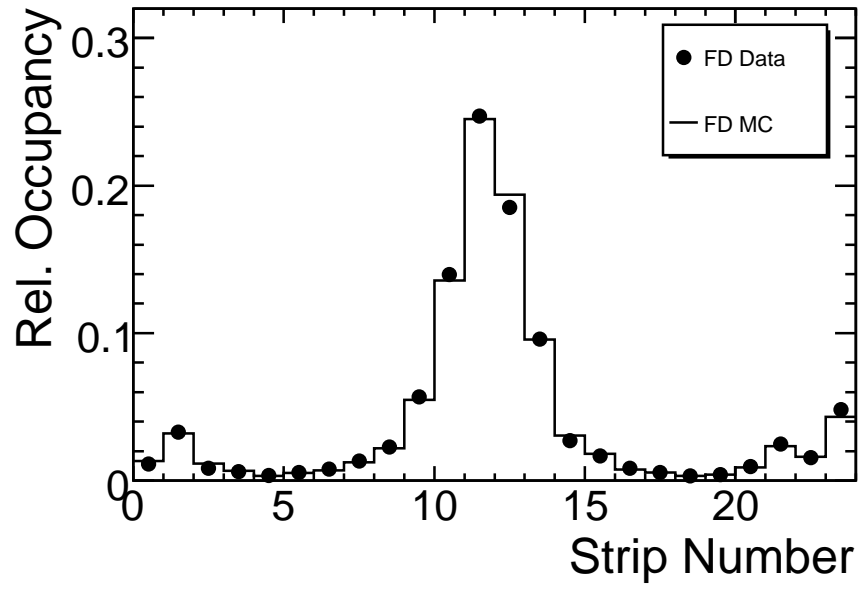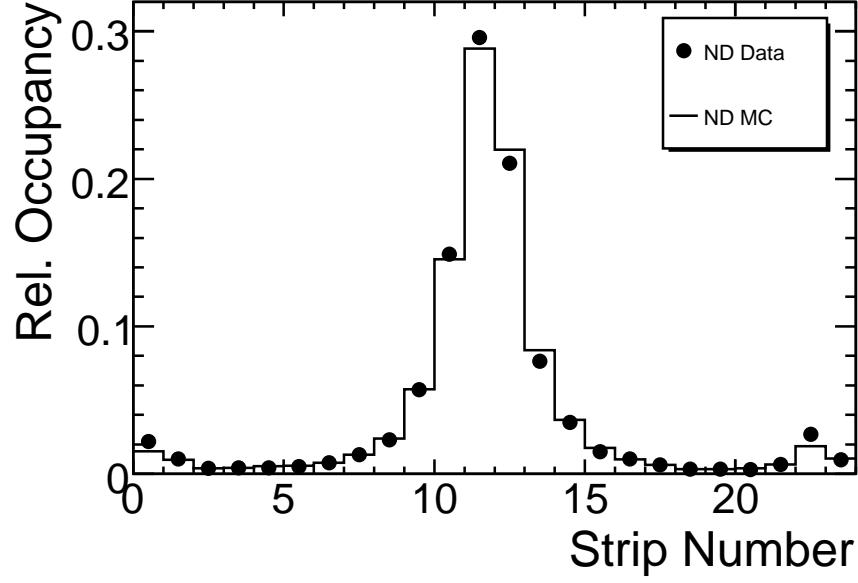
Figure 4: Transverse hit profile of >2 GeV/c test beam muons as measured with the ND (top) and FD (bottom) readout systems for data and MC. The central peak is mostly formed from strips that the muon actually passed through. Whereas, in contrast, the peaks towards the edges of the detector (strip number 0‑3 and 20‑23) are dominated by crosstalk hits. These data are from planes with strips that run horizontally.

was required. In contrast, strips with a response at just one end were included in the event-by-event comparison. Depending on the particle energy, approximately 90 - 95% of the total event energy comes from strips with a hit on both ends. The remainder comes from strips with a response on only one end and that fraction is consistent with PMT crosstalk, fluctuations in the production of photoelectrons, and readout thresholds.

7.1. Hit-by-hit Response Comparison

The average hit-by-hit asymmetry, $<A_{\mathcal{N}/\mathcal{F}}^{Hit}>$, is shown in Fig. 5 as a function of energy deposition. The data from positrons of between 0.6 - 6.0 GeV/c were used to cover the range of energy depositions from 0 - 36 MEU. The uniformity correction forces the asymmetry to be zero at around 1.5 MEU, which is the average energy deposition per strip of the cosmic ray muons used for the calibration of CalDet. Variation of $< A_{\mathcal{N}/\mathcal{F}}^{Hit} >$ as a function of energy deposition is best described by considering 2 distinct regions: above and below 4 MEU.

$<A_{\mathcal{N}/\mathcal{F}}^{Hit}>$ changes by up to 2% below 4 MEU with data and MC agreeing to 1%. The general trend is that $< A_{\mathcal{N}/\mathcal{F}}^{Hit} >$ increases by about 1.5% between 0.5 - 4 MEUs of energy deposited, which means that the ND response is increasing faster with energy deposited than the FD response. This variation is caused by the difference in the way the readout threshold is applied for the two readout systems: the ND electronics applies a threshold to each 18.8 ns integration sample separately, whereas the FD electronics only applies a threshold to the total integration sample (see Section 2 for more details). As the energy deposited increases, the fraction below readout threshold tends towards zero and so this effect is no longer significant. This trend is well described by the MC simulation, which shows a maximal deviation of less than 0.6% from the data in all but the lowest energy bin.

Between 4 - 15 MEU the slope goes the opposite way with $< A_{\mathcal{N}/\mathcal{F}}^{Hit} >$ decreasing with energy deposited by 2.5%. This is caused by the fact that the ND PMTs are less linear than the FD PMTs, as shown in Fig. 3. For energy depositions between 18 - 36 MEU, the trend is reversed with the slope of $< A_{\mathcal{N}/\mathcal{F}}^{Hit} >$ becoming positive again. The location of this inflection is consistent with the light level at which the FD readout system non-linearity starts to increase faster than that of the ND (see Fig. 3). The data and MC agreement in the region between 4 - 36 MEU is better than 1%. It is important to note that the results in this region quantify the maximum error
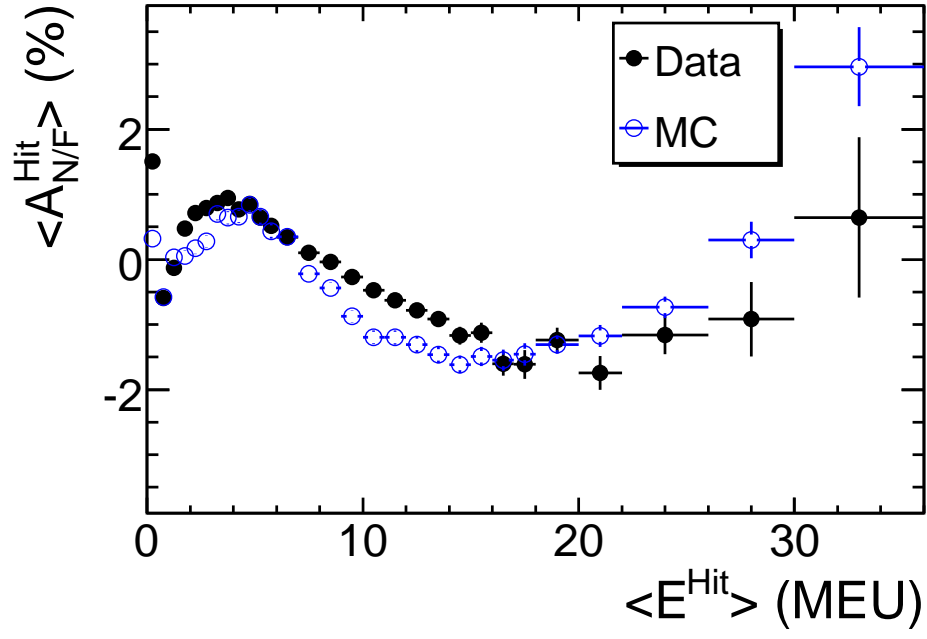
Figure 5: Average hit-by-hit asymmetry ratio, $< A^{Hit}_{\mathcal{N}/\mathcal{F}} >$, as a function of the average energy deposition in the scintillator strip hit for data and MC. It can be seen that difference between the response of ND and FD readout systems changes by up to 2.5% depending on the energy deposition.

in the case when a non-linearity correction was not applied. Whereas, when a non-linearity correction is applied the differences between the two readout systems at energy depositions above 4 MEU will be reduced.

In summary, the hit-by-hit data presented here show energy dependent differences between the calorimetric response of the two readout systems. These differences are shown to be caused by threshold effects as well as PMT and electronics non-linearity. The fact that the differences in the two readout systems are well simulated is particularly important for the relative calibration between the MINOS detectors. This result shows that as long as data and MC are made to agree at the energy of the muons used for calibration (around 1.5 MEU) then the MC can be used to correct for the relative differences between the ND and FD readout systems.

7.2. Event-by-Event Response Comparison

To make the comparison of the event-by-event response of the two readout systems, data from test beam positrons between 0.6 - 6.0 GeV/c were used. Fig. 6 shows the average event-by-event asymmetry, $<A_{\mathcal{N}/\mathcal{F}}^{Event}>$, as a function of the test beam momentum. It can be seen that there is no significant energy dependence. This is an important demonstration that the differences between the two readout systems seen in the hit-by-hit comparison do not introduce an overall **relative** energy dependent bias between the ND and FD (despite the absence of a non-linearity correction in the data presented here). It should be noted that a correction of 2.0% for the difference in crosstalk between the two readout systems was made in data and MC (see Section 6).

The average value of $<A_{\mathcal{N}/\mathcal{F}}^{Event}>$ between 0.6 - 6.0 GeV/c is

$$1.2 \pm 1.3\% \ \text{for data, and}$$
$$0.3 \pm 0.3\% \ \text{for MC.}$$

The statistical errors on both data and MC are negligible. The systematic uncertainties arise from the following sources: the uncertainty in the test beam position used to make the attenuation correction; the correction for differing quantities of crosstalk associated with strips; and bias in the uniformity correction.

The uncertainty on the position of the centre of the test beam in both data and MC gives a 0.25% error on $< A_{\mathcal{N}/\mathcal{F}}^{Event} >$. The uncertainty on the difference in the cross talk between the two readout systems gives a 0.14% error. For MC the systematic error from the uniformity correction is by
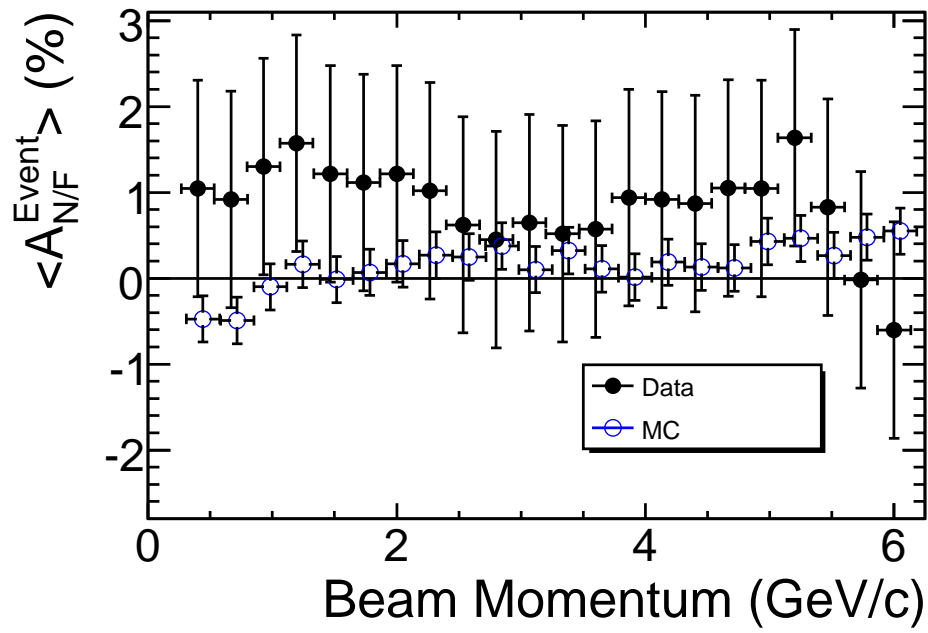
17

Figure 6: Average event-by-event asymmetry ratio, $< A_{\mathcal{N}/\mathcal{F}}^{Event} >$, as a function of the test beam momentum. The error bars show the total systematic error (statistical errors are negligible).

definition zero since the same calibration constants are used to both induce differences between the response of the strips in the simulation and then to calibrate out those differences.

For data the systematic uncertainty is dominated by the uniformity calibration. In order to estimate the systematic uncertainty on the uniformity calibration muons from the test beam with a momentum of more than 2 GeV/c were used. The value of $< A^{Hit}_{\mathcal{N}/\mathcal{F}} >$ obtained using these muons is shown as a function of position along the detector in Fig. 7. The data show a 1.1% difference between the first third of the detector and the back two thirds. In contrast, the asymmetry in the MC simulation is close to uniform throughout as expected. The presence of the asymmetry at the front of the detector in data is attributed to a bias induced by the uniformity correction. The measured asymmetry value of 1.1% is used as an estimate of the systematic error on the uniformity calibration and is the dominant error on $< A^{Hit}_{\mathcal{N}/\mathcal{F}} >$.

7.3. Readout System Resolution

The data described in this paper were obtained with the scintillator strips instrumented at one end with the ND readout system and at the other end by the FD system. The advantage of this approach was that it made the comparison of the two systems insensitive to fluctuations in the energy loss of the particles themselves and the simulation of such fluctuations in the MC. The fluctuations observed in $A^{Event}_{\mathcal{N}/\mathcal{F}}$ from event to event are due to fluctuations in the detector readout and the absorption/re-emission of photons in the WLS fibre. The dominant source of fluctuations arises in the conversion of photons to photoelectrons at the PMT face. For example, a 1 GeV/c positron yields about 180 PE and leads to a 15% width. The width of the distribution of $A^{Event}_{\mathcal{N}/\mathcal{F}}$ is shown in Fig. 8 as a function of positron momentum. It can be seen that the size of the fluctuations decreases with energy and is well reproduced by the MC simulation.

8. Conclusions

The MINOS Calibration detector has acquired test beam data in a configuration that allowed direct comparison of the two different readout systems used for the Near and Far detectors. These data were used to understand the systematic differences between the readout systems and to demonstrate that
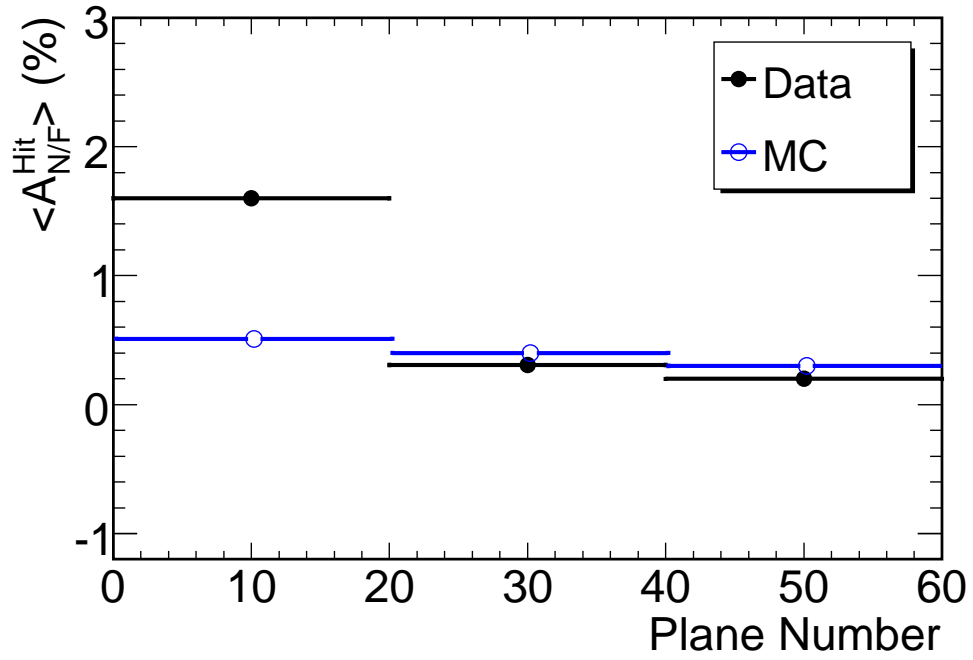
Figure 7: $< A_{\mathcal{N}/\mathcal{F}}^{Hit} >$ computed with test beam through going muons along the detector axis (statistical errors only). Data exhibits a difference in $< A_{\mathcal{N}/\mathcal{F}}^{Hit} >$ between the first third and the rest of the detector, which is consistent with calibration systematic bias.
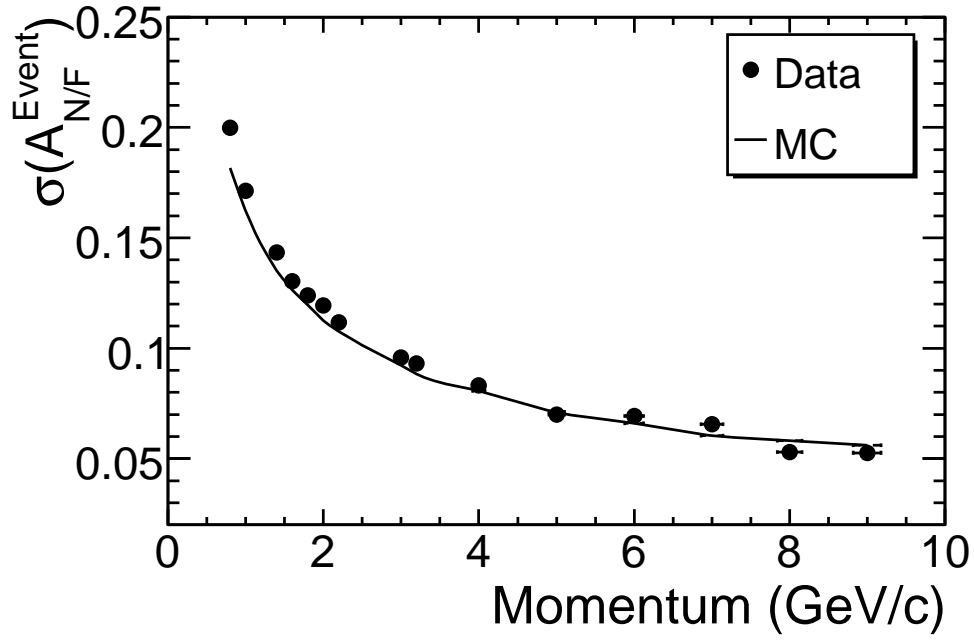
Figure 8: The readout system resolution (width of $A_{\mathcal{N}/\mathcal{F}}^{Event}$) as a function of positron momentum. This figure demonstrates the size of the fluctuations that occur in the readout when the same physics event is observed by both Near and Far systems. It can be seen that the size of the fluctuations decreases with energy and is well reproduced by the MC simulation.

the differences can be controlled to the level required by MINOS for neutrino oscillation measurements.

The results for the hit-by-hit calorimetric response comparison can be divided into two regions: energy depositions above and below 4 MEU. The relative hit-by-hit response of the two readout systems below 4 MEU changes by up to 2% with the MC reproducing the trend to 1%. The cause for this difference is demonstrated to be dominated by threshold effects in the electronics. This affect could potentially bias the relative energy calibration in MINOS. One way to avoid this bias is to calibrate the MC so that it agrees with the data in each detector separately. Above about 4 MEU the hit-by-hit response of the two systems differs by up to 2.5% with the MC reproducing the trends to better than 1%. This 2.5% variation is caused by differences in the non-linearity of the two types of PMT and electronics used for the Near and Far detectors.

The event-by-event comparison showed that the differences in the overall calorimetric response of the two readout systems were consistent with zero to an accuracy of 1.3% and 0.3% for data and MC respectively. Furthermore, no significant energy dependence was observed in positron data sets taken with test beam momentum settings between 0.6 - 6 GeV/c.

Differences in strip occupancy were shown to arise due to effects of crosstalk between pixels on the two types of multi-anode photomultiplier tubes used. This crosstalk, which is different for the two readout systems was demonstrated to be well reproduced by the MC simulation: both in the fraction of the total energy deposition dispersed as crosstalk and in its distribution across the pixels.

In the MINOS Near and Far detectors it is neutrino interactions that are reconstructed and that involves a multiplicity of particles in the hadronic shower. However, it is the combination of the result presented here for single positrons and the demonstrated accuracy of the MC simulation that is most important. These two results combined give confidence that any effects arising from the two different readout systems will be small enough so that they do not significantly impact the neutrino oscillation measurements made by MINOS.

9. Acknowledgements

References

[1] K. Anderson et al., NuMI Facility Technical Design Report, Technical Report, FERMILAB-DESIGN-1998-01, Fermilab, 1998.

[2] D. G. Michael et al., Nucl. Inst. & Meth. A596 (2008) 190-228.

[3] P. Adamson et al., Phys. Rev. Lett. 101, 131802 (2008).

[4] P. Adamson et al., Nucl. Inst. & Meth. A556 (2006) 119-133.

[5] A. Cabrera, Ph.D. Thesis, "Systematic Comparison of the MINOS Near and Far Detector Readout Systems", University of Oxford, Fermilab-Thesis-2005-50, 2005.

[6] N. Tagg et al., Nucl. Inst. & Meth. A539 (2005) 668-678.

[7] T. Cundiff et al., IEEE Trans. Nucl. Sci. 53 (2006) 1346.

[8] K. Lang et al., Nucl. Inst. & Meth. A545 (2005) 852-871.

[9] J. Oliver et al., IEEE Trans. Nucl. Sci. 51 (2004) 2193-2195.

[10] L. Durieu et al., in IEEE "Proceeding of the Particle Accelerator Conference, 1997", Vol. 1, pages 228-230.

[11] M.A. Kordosky, Ph.D. Thesis, "Hadronic interactions in the MINOS detectors", University of Texas at Austin, Fermilab-Thesis-2004-34, 2004.

[12] T.A. Gabriel et al., Nucl. Inst. & Meth. A349 (1994) 106.

[13] P. Adamson et al., Nucl. Inst. & Meth. A492 (2002) 325-343 and A521 (2004) 361-366.

[14] J.J. Hartnell, Ph.D. Thesis, "Measurement of the calorimetric energy scale in MINOS", University of Oxford, Fermilab-Thesis-2005-51, 2005.